Head and Neck Tumors: Assessment of Perfusion-Related Parameters and Diffusion Coefficients Based on the Intravoxel Incoherent Motion Model

M. Sumi and T. Nakamura

ABSTRACT

BACKGROUND AND PURPOSE: IVIM MR imaging provides perfusion and diffusion information with a single diffusion-weighted MR image. We determined whether PP and D differ among various types of head and neck tumors.

MATERIALS AND METHODS: The study cohort included 123 head and neck tumors: 30 SCCs, 28 benign and 20 malignant SG tumors, 36 lymphomas, and 9 schwannomas. The D and PP values were determined by using b-values of 0, 500, and 1000 s/mm^2 based on the IVIM model.

RESULTS: The PP values (lymphomas, 0.09 $\pm$ 0.04; SCCs, 0.15 $\pm$ 0.04; and malignant SG tumors, 0.22 $\pm$ 0.07) and D values (0.47 $\pm$ 0.07 $\times$ 10^{-3} mm^2/s, 0.82 $\pm$ 0.17 $\times$ 10^{-3} mm^2/s, and 1.03 $\pm$ 0.16 $\times$ 10^{-3} mm^2/s, respectively) were significantly different among the malignant tumors ($P < .01$). These values were also significantly different between pleomorphic adenomas (0.13 $\pm$ 0.02 and 1.44 $\pm$ 0.39 $\times$ 10^{-3} mm^2/s) and Warthin tumors (0.19 $\pm$ 0.04 and 0.73 $\pm$ 0.22 $\times$ 10^{-3} mm^2/s) ($P < .001$). The PP values of malignant SG tumors were significantly different from those of pleomorphic adenomas ($P = .001$) and the D values of the malignant SG tumors were significantly different from those of pleomorphic adenomas ($P = .002$) and Warthin tumors ($P = .007$). Schwannomas had large PP (0.23 $\pm$ 0.08) and D values (1.26 $\pm$ 0.20 $\times$ 10^{-3} mm^2/s), greatly overlapping those of some SG tumor types.

CONCLUSIONS: Head and neck tumors had distinctive PP and D values by using IVIM MR imaging.

ABBREVIATIONS: D = diffusion coefficient; D* = perfusion-related incoherent microcirculation; f = perfusion factor; IVIM = intravoxel incoherent motion; PP = perfusion-related parameter; SCC = squamous cell carcinoma; SG = salivary gland

DWI can estimate the Brownian motion of intracellular and extracellular water molecules. It is based on the displacement of water molecules that are allowed to migrate for a given time.[1,2] The movement of water molecules is impeded by the presence of cells, membranes, and extracellular and intracellular macromolecules. In biologic tissues, however, DWI is also affected by microcirculation of blood in the capillaries. Water proton mobility can be characterized by ADC. However, this parameter cannot separate the pure molecular diffusion from the motion of water molecules in the capillary network. IVIM imaging can quantitate molecular diffusion and microcirculation in the capillary network in a single-image voxel at MR imaging.[3] Le Bihan et al [4] and Luciani et al[5] demonstrated that IVIM imaging can distinguish between the pure molecular diffusion and motion of water molecules in the capillary network with a single DWI acquisition technique, provided that large b-values encompassing both low b-values (<200 s/mm^2) and high b-values (>200 s/mm^2) are used.

Recently, several attempts have been made to determine the perfusion and diffusion parameters separately by using IVIM MR imaging.[5-7] The diffusion properties of tumor tissues largely depend on cell attenuation. Some studies have shown that ADCs are useful for predicting malignancy (eg, metastatic nodes in the necks of patients with SCC and salivary gland tumors).[8,9] However, this concept has not yet been established.[10] Perfusion is a very important marker of many physiologic or pathologic processes. For example, the perfusion parameter can be used as a biomarker for predicting the responsiveness of some types of tumors to chemotherapy.[11,12] Therefore, estimating these 2 distinctive phenomena in tumor tissues may be helpful in the preoperative characterization of tumors.

A simplified IVIM MR imaging technique based on the IVIM model was used to assess the PP and D of hepatocellular carcinomas.[12] In that study, the PP was determined with 4 b-values (0, 200, 400, and 800 s/mm^2), a technique that is easy to apply and fast

Received February 29, 2012; accepted after revision May 19.

From the Department of Radiology and Cancer Biology, Nagasaki University School of Dentistry, Nagasaki, Japan.

Please address correspondence to Takashi Nakamura, DDS, PhD, Department of Radiology and Cancer Biology, 1-7-1 Sakamoto, Nagasaki 852-8588, Japan; e-mail: taku@nagasaki-u.ac.jp

http://dx.doi.org/10.3174/ajnr.A3227

Tumor types, histologic types, and locations of 123 head and neck tumors

Tumor Types	No.	Locations	No.
SCC	30	Tongue	12
		Gingiva	10
		Oropharynx	3
		Oral floor	2
		Buccal mucosa	1
		Hypopharynx	1
		Paranasal sinus	1
SG tumor			
Benign	28	Parotid gland	10
Pleomorphic adenoma		Submandibular gland	3
		Minor salivary gland	2
Warthin tumor		Parotid gland	13
Malignant[a]	20	Parotid gland	7
		Submandibular gland	3
		Sublingual gland	3
		Minor salivary gland	3
		Mandible	2
		Paranasal sinus	2
Lymphoma	36	Lymph node	19
		Oropharynx	3
		Nasal cavity	3
		Paranasal sinus	2
		Thyroid gland	2
		Parotid gland	2
		Parapharyngeal space	2
		Nasopharynx	1
		Mandible	1
		Submandibular space	1
Schwannoma	9	Carotid space	7
		Buccal space	1
		Mandible	1

[a] Malignant SG tumors include adenoid cystic carcinoma ($n = 6$), adenocarcinoma ($n = 4$), mucoepidermoid carcinoma ($n = 3$), carcinoma ex pleomorphic adenoma ($n = 3$), epithelial-myoepithelial carcinoma ($n = 1$), myoepithelial carcinoma ($n = 1$), salivary duct carcinoma ($n = 1$), and acinic cell carcinoma ($n = 1$).

compared with the IVIM imaging by using multiple b-values (eg, 0, 10, 20, 30, 50, 80, 100, 200, 400, and 800 s/mm^2).[5]

In the present study, we characterized different types of head and neck tumors by assessing PP and D values on the basis of the IVIM model by using 3 b-values.

MATERIALS AND METHODS

Patients

We retrospectively analyzed IVIM MR images obtained from 118 patients with head and neck tumors who underwent preoperative MR imaging examinations between 2005 and 2010. Of these, 5 patients were excluded from the present study due to poor MR images (severe susceptibility and/or motion artifacts) or prior surgical intervention, such as excisional biopsy. Consequently, we studied diffusion-weighted MR images from 113 patients with head and neck tumors (51 women and 62 men; average age, 60 years; age range, 21–91 years). Eight patients with lymphoma had multiple lesions (1 patient had 4 lesions and 7 patients had 2 lesions each). Therefore, we studied IVIM images of 123 head and neck tumors having >10-mm short-axis diameters on contrast-enhanced T1-weighted MR images and comprising 30 SCCs, 28 benign and 20 malignant SG tumors, 36 lymphomas, and 9 schwannomas (Table). This retrospective study was approved by the institutional review board.

Conventional MR Imaging

MR imaging was performed by using a 1.5T MR imaging unit (Gyroscan Intera 1.5T Master; Philips Healthcare, Best, the Netherlands) with a 2-channel 11-cm (Synergy-Flex S), 17 × 14 cm (Synergy-Flex M), or 20-cm (Synergy-Flex L) surface coil or a 3-channel head and neck coil (Synergy; Philips Healthcare). We obtained axial T1-weighted (TR/TE/number of signal acquisitions = 500/15 ms/2) and fat-suppressed (spectral attenuated with inversion recovery) T2-weighted (TR/TE/number of signal acquisitions = 6385/80 ms/2) MR images by using a TSE sequence with a TSE factor of 3 (T1-weighted) or 15 (fat-suppressed T2-weighted). We used a 200-mm FOV, 256 × 204 scan and 512 × 512 reconstruction matrix sizes, a 4-mm section thickness, and a 0.4-mm section gap.

Contrast-Enhanced MR Imaging

Contrast-enhanced T1-weighted MR images were used as references for manually placing ROIs on DWI of head and neck tumors. Gadolinium (gadopentetate dimeglumine, Magnevist; Bayer Yakuhin, Osaka, Japan) was intravenously injected at a dose of 0.2 mL/kg body weight and at an injection rate of 1.5 mL/s, followed by a 20-mL saline flush.

Diffusion-Weighted Imaging

DWI was performed before the contrast-enhanced MR imaging. Axial DWI (TR/TE/number of signal acquisitions = 4283/87 ms/4) was obtained by using single-shot spin-echo EPI.[8,10] We used 3 b factors (0, 500, and 1000 s/mm^2). We obtained isotropic diffusion images by applying the 2 higher b factors along the 3 orthogonal directions by using a 200-mm FOV, 4-mm section thickness, 0.4-mm section gap, and 112 × 90 matrix size. Phase-encoding was applied along the anteroposterior direction. The surface coils were placed on the left and right sides of the neck, and the head and neck coil elements were placed on the anterior and posterior sides of the head and neck. The parallel imaging (sensitivity encoding factor = 2) technique was used for rapid image acquisition and reducing susceptibility artifacts. Imaging time was 2 minutes 8 seconds for the acquisition of 25 sections.

Region-of-Interest Placement

We analyzed DWI obtained at $b = 0$, 500, and 1000 s/mm^2. We used 1–3 sections from each tumor, depending on the tumor size. A region of interest was manually placed onto each tumor area of the DWI so that it encompassed as much of the tumor area as possible. Visually large cystic or necrotic areas were excluded. We used contrast-enhanced and nonenhanced T1-weighted MR images as references to determine tumor areas on the corresponding DWI. The IVIM values (PP and D) obtained from 1–3 sections from each tumor were averaged. A radiologist with 15 years' experience in head and neck radiology placed ROIs and analyzed DWI.

IVIM MR Imaging

The relationship between signal intensities and b-values was assessed on the basis of the IVIM theory by using the following equation:

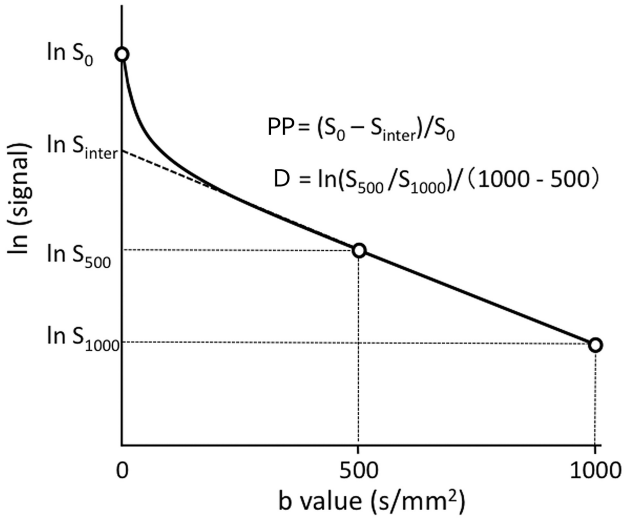

FIG 1. Perfusion-related parameter and diffusion coefficient as determined on the basis of the IVIM model. The PP is estimated by the equation PP = $(S_0 - S_{inter}) / S_0$. The D is calculated by the equation D = ln $(S_{500} / S_{1000})/ 500$. S_0 and S_{inter} are signal intensities at b=0 s/mm^2 and at the interception of the logarithmic regression line obtained by using b-values of 500 and 1000 s/mm^2 with the y-axis, respectively.

1)

$$S_b/S_0 = (1 - f) \cdot \exp(-bD) + f \cdot \exp[-b(D + D^*)],$$

where f is a microvascular volume fraction representing the fraction of diffusion linked to microcirculation,[5] D is the diffusion parameter representing pure molecular diffusion (diffusion coefficient), and D* is the perfusion-related incoherent microcirculation. S_0 and S_b are signal intensities at b=0 and b>0 s/mm^2, respectively (Fig 1). Because D* is much greater than D, the effects of D* on the signal at large b-values (>300 s/mm^2) can be neglected,[5] and equation 1 can be simplified as

2) $$S_{b1}/S_{b2} = \exp[(b_2 - b_1)D)],$$

where S_{b1} and S_{b2} are signal intensities at 2 different b-values.[8] Accordingly, by using logarithmic plots, D can be obtained with a linear regression algorithm. Given an estimated D value from equation 2, the corresponding f and D* values can be calculated by using a nonlinear regression algorithm based on equation 1.

However, the PPs can be determined as $1 - S_{inter} / S_0$ (S_{inter} is the interception of the logarithmic regression line obtained by using b-values of 500 and 1000 s/mm^2 with the y-axis) (Fig 1).[12] Therefore, we defined the PP value as signal decays due to quasi-random proton movement within the capillary network between b=0 and b=500 s/mm^2. In the present study, we evaluated tumor perfusion by using PP values and did not assess D* values.

Perfusion and Diffusion Maps

DWIs obtained at b=0, 500, and 1000 s/mm^2 in a DICOM format were transferred onto a personal computer (iMac; Apple, Cupertino, California) and were then analyzed by using ImageJ software (National Institutes of Health, http://rsbweb.nih.gov/ij). 2D distributions of the PP and D values were displayed as PP and D maps, respectively (Figs 2–6).

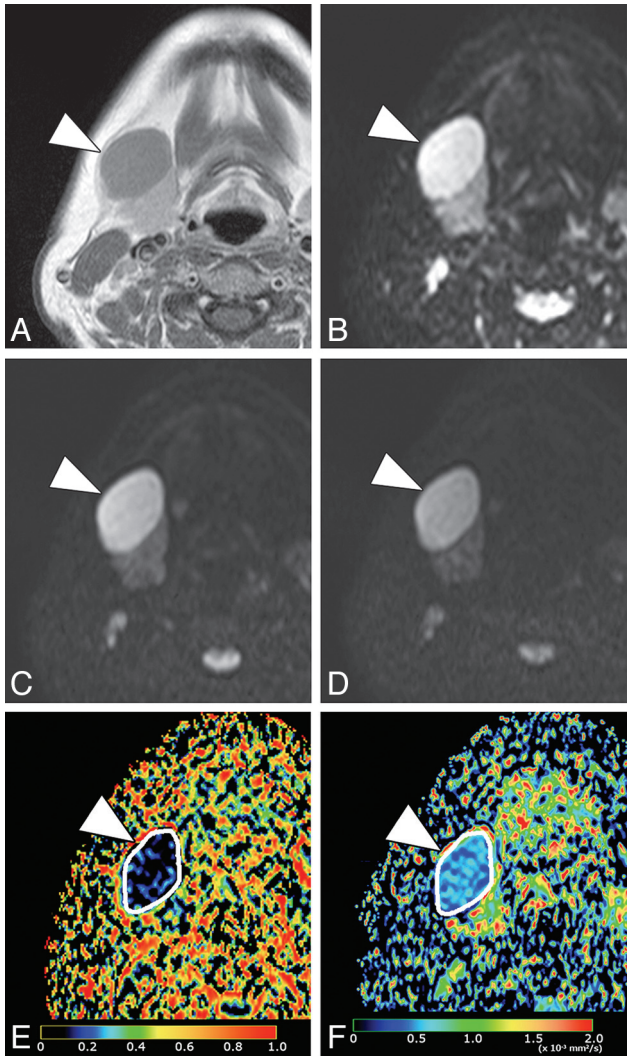

FIG 2. A 50-year-old woman with nodal lymphoma (follicular lymphoma). *A*, Axial contrast-enhanced T1-weighted image shows a homogeneously enhancing tumor (*arrowhead*) in the submandibular space. *B*, Axial DWI at b=0 s/mm^2. *C*, Axial DWI at b=500 s/mm^2. *D*, Axial DWI at b = 1000 s/mm^2. *E*, Axial PP map shows the tumor (*arrowhead*) with very small perfusion (average PP value = 0.05). The white contour indicates the tumor area on the map. *F*, Axial D map shows the tumor (*arrowhead*) with small diffusion (average D value = 0.53×10^{-3} mm^2/s). The white contour indicates the tumor area on the map.

Statistics

Kruskal-Wallis and Steel-Dwass tests were used for the comparison of the IVIM parameters among the 6 different types of head and neck tumors. Kruskal-Wallis and Steel-Dwass tests were performed by using Excel Statistics, Version 1.12 (Social Survey Research Information, Tokyo, Japan).

RESULTS

Perfusion-Related Parameters of Head and Neck Tumors

The PP values were significantly different among the 6 types of head and neck tumors ($P < .001$, Kruskal-Wallis test) (Figs 2–4 and 5*A*).

The Steel-Dwass test revealed that the PP values of lymphomas (0.09 ± 0.04) were the smallest among the different types of head and neck tumors examined (Figs 2 and 5*A*). The PP values of

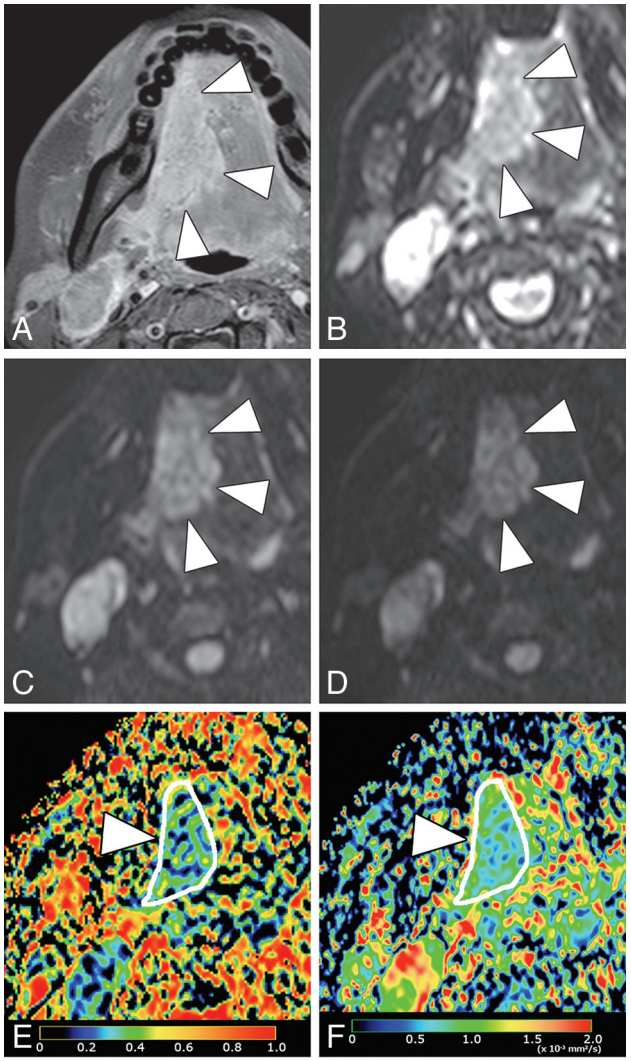

FIG 3. A 37-year-old woman with SCC in the tongue. *A*, Axial fat-suppressed contrast-enhanced T1-weighted image shows enhancing tumor (*arrowheads*), which occupies the right anterior two-thirds of tongue. *B*, Axial DWI at $b = 0$ s/mm^2. *C*, Axial DWI at $b = 500$ s/mm^2. *D*, Axial DWI at $b = 1000$ s/mm^2. *E*, Axial PP map shows the tumor (*arrowheads*) with small perfusion (average PP value = 0.14). *F*, Axial D map shows the tumor (*arrowhead*) with small diffusion (average D value = 0.68×10^{-3} mm^2/s).

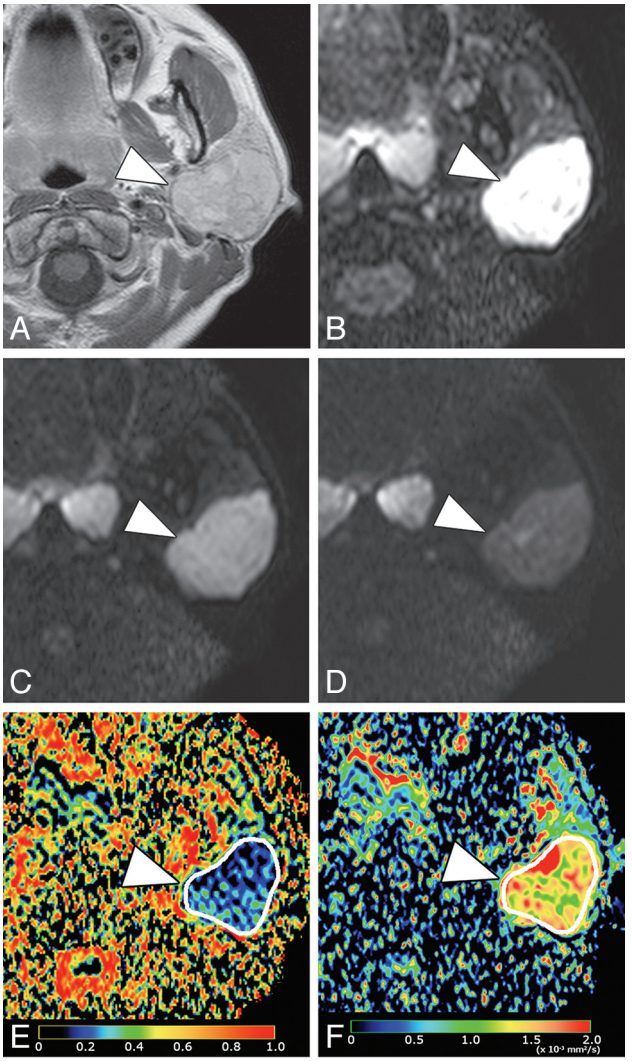

FIG 4. A 42-year-old woman with pleomorphic adenoma in the parotid gland. *A*, Axial contrast-enhanced T1-weighted image shows enhancing tumor (*arrowhead*) in the left parotid gland. *B*, Axial DWI at $b = 0$ s/mm^2. *C*, Axial DWI at $b = 500$ s/mm^2. *D*, Axial DWI at $b = 1000$ s/mm^2. *E*, Axial PP map shows the tumor (*arrowhead*) with small perfusion (average PP value = 0.13). *F*, Axial D map shows the tumor (*arrowhead*) with intermediate-to-large diffusion (average D value = 1.47×10^{-3} mm^2/s).

malignant SG tumors (0.22 ± 0.07) were the largest, and those of SCCs (0.15 ± 0.04) were intermediate among the 3 types of malignant tumors (Figs 3 and 5*A*).

Pleomorphic adenomas had the smallest PP values (0.13 ± 0.02) among the 3 types of SG tumors (Figs 4 and 5*A*). The PP values of schwannomas (0.23 ± 0.08) were significantly larger than those of pleomorphic adenomas but were similar to those of Warthin tumors (0.19 ± 0.04) (Fig 5*A*).

Diffusion Coefficients of Head and Neck Tumors

The D values were also significantly different among the 6 types of head and neck tumors ($P < .001$, Kruskal-Wallis test) (Figs 2–4, 5*B*).

The D values of lymphomas ($0.47 \pm 0.07 \times 10^{-3}$ mm^2/s) were the smallest among the different types of head and neck tumors examined (Figs 2 and 5*B*) (Steel-Dwass test). The D values of malignant SG tumors ($1.03 \pm 0.16 \times 10^{-3}$ mm^2/s) were the largest, and those of SCCs were intermediate ($0.82 \pm 0.17 \times 10^{-3}$ mm^2/s) among the 3 types of malignant tumors (Figs 3 and 5*B*).

The D values were significantly different among the 3 types of SG tumors (Steel-Dwass test); pleomorphic adenomas had the largest ($1.44 \pm 0.39 \times 10^{-3}$ mm^2/s) and Warthin tumors had the smallest ($0.73 \pm 0.22 \times 10^{-3}$ mm^2/s) values (Figs 4 and 5*B*). Furthermore, the D values of pleomorphic adenomas were the largest among the different head and neck tumors examined, but the values were similar to those of schwannomas ($1.26 \pm 0.20 \times 10^{-3}$ mm^2/s) (Fig 5*B*).

Flow-Related Fraction and Diffusion Properties of Head and Neck Tumors

Figure 6 shows the 2D distributions of PP and D values of the head and neck tumors. Lymphomas had low PP (<0.15) and D

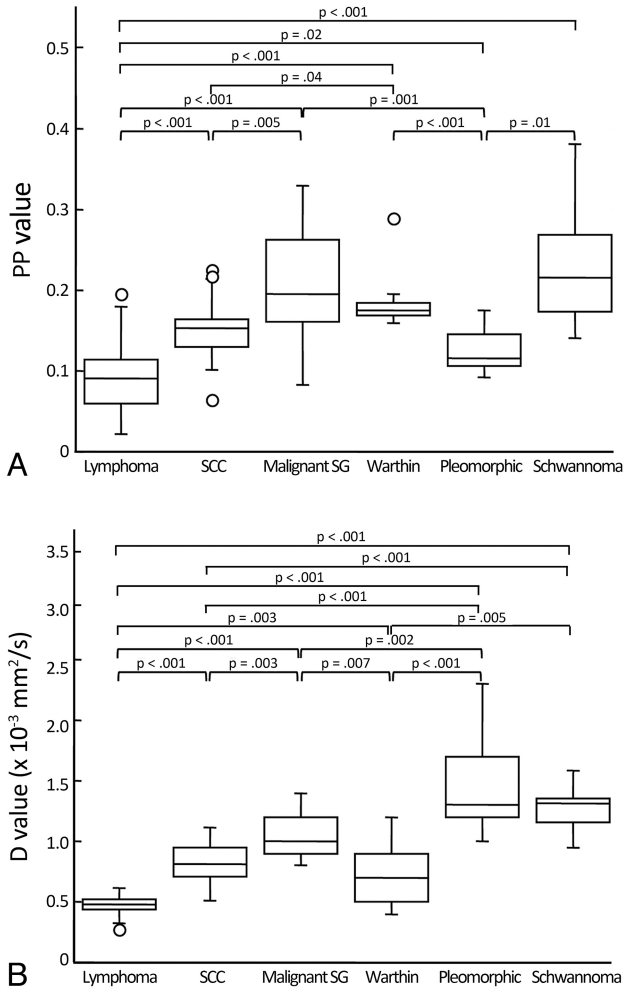

FIG 5. Boxplots show PP (*A*) and D (*B*) values of head and neck tumors. The horizontal line is a median (50th percentile) of the measured values; the top and bottom of the box represent the 25th and 75th percentiles, respectively; and whiskers indicate the range from the largest and smallest observed data within the 1.5 interquartile range presented by the box. P indicates the Steel-Dwass test. Plots demonstrated as open circles indicate outliers. Warthin indicates Warthin tumor; Pleomorphic, pleomorphic adenoma.

($<1.0 \times 10^{-3}$ mm^2/s) values. Pleomorphic adenomas also had high PP values; however, their D values were high ($>1.0 \times 10^{-3}$ mm^2/s) and varied greatly. SCCs and Warthin tumors had low-to-high f (>0.15) values and low D values. Malignant SG tumors had broad-range low-to-high PP values and narrow-range low-to-high D values. The PP values of schwannomas were broad-range and similar to those of malignant SG tumors, but their D values were high.

DISCUSSION

We characterized benign and malignant head and neck tumors by using perfusion-related (PP) and purely molecular-based (D) diffusion parameters based on the IVIM model. The present study demonstrated that different types of head and neck tumors had distinct IVIM profiles consisting of varying proportions of capillary perfusion and pure molecular diffusion components.

Malignant salivary gland tumors, Warthin tumors, and schwannomas had large PP values among the head and neck tumors examined. The PP values of SCCs were intermediate, and those of lymphomas were the smallest among the head and neck tumors examined. These results may be attributed to the differences in histologic structure (in particular, differences in the relative area of stromal tissues) among these tumors. Malignant salivary gland tumors are composed of cancer cell nests within varying amounts of stromal tissues, which may be associated with abundant vessels.[13] Schwannomas are composed of cellular Antoni A areas with Verocay bodies and hypocellular myxoid Antoni B areas. Small vessels with ectasia are frequently observed in the Antoni B areas. On the other hand, lymphomas exclusively comprised condensed proliferating lymphoma cells, with scarce amounts of stromal tissues between the tumor cells.[14] SCCs are associated with varying degrees of deposition of extracellular matrix; under these conditions, neovascularization frequently occurs. Therefore, the perfusion level of the tumor may represent the relative area of stromal tissues with varying levels of vessel attenuation to the overall tumor area.

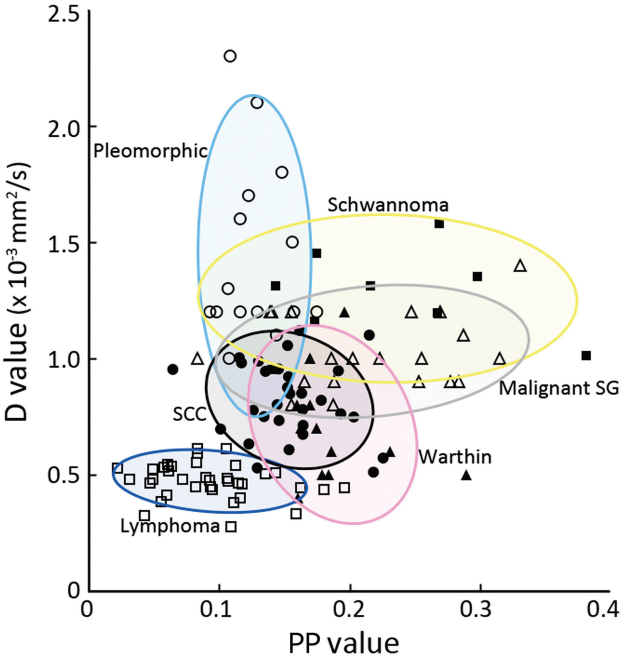

FIG 6. 2D distributions of PP and D values of head and neck tumors. Lymphomas (*open squares*), pleomorphic adenomas (*open circles*), schwannomas (*open triangles*), malignant SG tumors (*closed squares*), SCCs (*closed circles*), and Warthin tumors (*closed triangles*). Each oblong area indicates a PP/D value area that encompasses 80% of a particular type of head and neck tumor.

The diffusion coefficient level is largely dependent on the ratios of the intracellular and extracellular spaces of tumors.[4] The observed differences in D values among the benign and malignant tumors examined are consistent with this notion; tumors with large areas of stromal tissues appear to exhibit higher D values. The levels of tumor PP values do not correlate with those of tumor D values. For example, the D values of pleomorphic adenomas were significantly higher than those of Warthin tumors and malignant salivary gland tumors; however, the PP values of pleomorphic adenomas were significantly lower than those of Warthin tumors and malignant salivary gland tumors. These results are

consistent with the notion that tumors have distinctive stromal components with varying degrees of vascularization.

The perfusion levels in head and neck tumors may be dependent on the tumor microvessel attenuation.[15] The PP value is determined as the signal intensity ratios of blood capillaries and tumor tissues. However, T2 contributions from tumor tissues and blood capillaries may differ greatly.[16] Therefore, one should be careful with the interpretation of f in tumors. A prolonged T2 of the tissue will lead to an increasingly lower calculated value of PP.

Inconsistent with the present results, a study by using perfusion CT imaging showed that blood volumes of malignant salivary gland tumors were significantly lower than those of benign salivary gland tumors.[17] In the present study, however, we found that the f values of malignant salivary gland tumors were significantly higher than those of pleomorphic adenomas. The discrepancy between these studies implies that the tumor perfusion estimated on the basis of contrast-enhanced imaging techniques differs from the tumor perfusion estimated on the basis of the DWI technique.

In the present study, we used 3 b-values (0, 500, and 1000 s/mm^2) to determine the PP values on the basis of the IVIM model. However, more b-values $<$300 s/mm^2 could be used to simulate the biexponential IVIM model to estimate tumor perfusion more accurately. Recently, in an attempt to differentiate between patients with liver cirrhosis and those without liver fibrosis, Luciani et al[5] used 10 b factors (0, 10, 20, 30, 50, 80, 100, 200, 400, and 800 s/mm^2) to calculate pure molecular-based and perfusion-related diffusion parameters. Therefore, further studies on a larger cohort comprising a broader spectrum of head and neck tumors should be conducted by using DWI with increased numbers of b-values $<$300 s/mm^2 to determine the clinical usefulness of assessing perfusion characteristics of head and neck tumors on the basis of the IVIM model. Another limitation of this study is that we did not perform cross-validation with established perfusion techniques, such as CT perfusion, arterial spin-labeling, dynamic susceptibility contrast MR imaging, and/or dynamic contrast-enhanced MR imaging.[18-20] Future cross-validation studies are required to establish the usefulness of the IVIM parameters in assessing the perfusion characteristics of head and neck tumors.

IVIM MR imaging could potentially be used as a technique for predicting the prognosis of patients with head and neck tumors. Hermans et al[21] and, more recently, Zima et al[11] and Bisdas et al[22,23] demonstrated that CT-determined tumor perfusion efficiently predicted the local outcomes of patients with head and neck cancer who received radiation therapy or chemoradiotherapy. These previous studies suggest that perfusion levels of head and neck tumors determine the tumor responsiveness to chemoradiotherapy. Therefore, perfusion studies by using IVIM imaging and contrast-enhanced CT may be useful for predicting the efficacy of chemoradiotherapy in patients with head and neck SCCs, thereby predicting the prognosis of patients with those SCCs.

Previous studies have also shown that the diffusion coefficients could serve as the criteria for differentiating between benign and malignant salivary gland tumors as well as between lymphomas and SCCs in the pharynx.[9,24] The results of the present study support the clinical feasibility of using non-contrast-enhanced perfusion MR imaging as a diagnostic tool for differentiating benign and malignant tumors and even for differentiating among different types of malignant tumors in the head and neck. Furthermore, the combined use of PP and D values of tumors might potentiate the clinical use of DWI.

The PP and D values were much overlapped among different types of head and neck tumors as shown in Fig 6. However, these values may be useful in differentiating among some types of head and neck tumors, for example between benign and malignant salivary gland tumors. In addition, this simplified technique for simultaneously assessing perfusion and diffusion characteristics is easy to use and fast. Therefore, a combined use of PP and D values obtained with DWI could be an adjunct to conventional MR imaging for preoperatively diagnosing different types of head and neck tumors.

CONCLUSIONS

We demonstrated that head and neck tumors have distinctive perfusion-related parameters and diffusion coefficients by using IVIM MR imaging. Characterization of both perfusion and diffusion properties of head and neck tumors could be achieved by using a single DWI study with multiple b-values.

REFERENCES

1. Padhani AR, Liu G, Mu-Koh D, et al. **Diffusion-weighted magnetic resonance imaging as a cancer biomarker: consensus and recommendations.** *Neoplasia* 2009;11:102–25
2. Le Bihan D. **Looking into the functional architecture of the brain with diffusion MRI.** *Nat Rev Neurosci* 2003;4:469–80
3. Le Bihan D, Breton E, Lallemand D, et al. **MR imaging of intravoxel incoherent motions: application to diffusion and perfusion in neurologic disorders.** *Radiology* 1986;161:401–07
4. Le Bihan D, Breton E, Lallemand D, et al. **Separation of diffusion and perfusion in intravoxel incoherent motion MR imaging.** *Radiology* 1988;168:497–505
5. Luciani A, Vignaud A, Cavet M, et al. **Liver cirrhosis: intravoxel incoherent motion MR imaging—pilot study.** *Radiology* 2008;249:891–99
6. Moteki T, Horikoshi H. **Evaluation of hepatic lesions and hepatic parenchyma using diffusion-weighted echo-planar MR with three values of gradient b-factor.** *J Magn Reson Imaging* 2006;24:637–45
7. Coenegrachts K, Delanote J, Ter Beek L, et al. **Evaluation of true diffusion, perfusion factor, and apparent diffusion coefficient in non-necrotic liver metastases and uncomplicated liver hemangiomas using black-blood echo planar imaging.** *Eur J Radiol* 2009;69:131–38
8. Sumi M, Nakamura T. **Diagnostic importance of focal defects in the apparent diffusion coefficient-based differentiation between lymphoma and squamous cell carcinoma nodes in the neck.** *Eur Radiol* 2009;19:975–81
9. Eida S, Sumi M, Sakihama N, et al. **Apparent diffusion coefficient mapping of salivary gland tumors: prediction of the benignancy and malignancy.** *AJNR Am J Neuroradiol* 2007;28:116–21
10. Habermann CR, Arndt C, Graessner J, et al. **Diffusion-weighted echo-planar MR imaging of primary parotid gland tumors: is a prediction of different histologic subtypes possible?** *AJNR Am J Neuroradiol* 2009;30:591–96
11. Zima A, Carlos R, Gandhi D, et al. **Can pretreatment CT perfusion predict response of advanced squamous cell carcinoma of the upper aerodigestive tract treated with induction chemotherapy?** *AJNR Am J Neuroradiol* 2007;28:328–34
12. Lewin M, Fartoux L, Vignaud A, et al. **The diffusion-weighted imaging perfusion fraction f is a potential marker of sorafenib treatment**

in advanced hepatocellular carcinoma: a pilot study. *Eur Radiol* 2011;21:281–90
13. Barnes L, Eveson JW, Reichart P, et al. *Pathology and Genetics of Head and Neck Tumours*. Lyon, France: IARC Press; 2005
14. Swerdlow SH, Campo E, Harris NL, et al. *WHO Classification of Tumours of Haematopoietic and Lymphoid Tissues*. 4th ed. Lyon, France: IARC Press; 2008
15. Ash L, Teknos TN, Gandhi D, et al. **Head and neck squamous cell carcinoma: CT perfusion can help noninvasively predict intratumoral microvessel density.** *Radiology* 2009;251:422–28
16. Clark CA, Le Bihan D. **Water diffusion compartmentation and anisotropy at high b values in the human brain.** *Magn Reson Med* 2000;44:852–59
17. Bisdas S, Baghi M, Wagenblast J, et al. **Differentiation of benign and malignant parotid tumors using deconvolution-based perfusion CT imaging: feasibility of the method and initial results.** *Eur J Radiol* 2007;64:258–65
18. Abdel Razek A, Gaballa G. **Role of perfusion magnetic resonance imaging in cervical lymphadenopathy.** *J Comput Assist Tomogr* 2011;35:21–25
19. Schraml C, Boss A, Martirosian P, et al. **FAIR true-FISP perfusion imaging of the thyroid gland.** *J Magn Reson Imaging* 2007;26:66–71
20. Shah G, Wesolowski J, Ansari S, et al. **New directions in head and neck imaging.** *J Surg Oncol* 2008;97:644–48
21. Hermans R, Meijerink M, Van den Bogaert W, et al. **Tumor perfusion rate determined noninvasively by dynamic computed tomography predicts outcome in head-and-neck cancer after radiotherapy.** *Int J Radiat Oncol Biol Phys* 2003;57:1351–56
22. Bisdas S, Rumboldt Z, Šurlan-Popovič K, et al. **Perfusion CT in squamous cell carcinoma of the upper aerodigestive tract: long-term predictive value of baseline perfusion CT measurements.** *AJNR Am J Neuroradiol* 2010;31:576–81
23. Bisdas S, Nguyen SA, Anand SK, et al. **Outcome prediction after surgery and chemoradiation of squamous cell carcinoma in the oral cavity, oropharynx, and hypopharynx: use of baseline perfusion CT microcirculatory parameters vs. tumor volume.** *Int J Radiat Oncol Biol Phys* 2009;73:1313–18
24. Sumi M, Ichikawa Y, Nakamura T. **Diagnostic ability of apparent diffusion coefficients for lymphomas and carcinomas in the pharynx.** *Eur Radiol* 2007;17:2631–37